J Fluoresc (2010) 20:797–808
DOI 10.1007/s10895-010-0606-4

ORIGINAL PAPER

Rotational Diffusion of Coumarins: A Dielectric Friction Study

J. R. Mannekutla · Sanjeev R. Inamdar · B. G. Mulimani · M. I. Savadatti

Received: 16 November 2009 / Accepted: 29 January 2010 / Published online: 2 March 2010

Abstract The rotational diffusion of three probes: coumarin 522B (C522B), coumarin 307 (C307) and coumarin 138 (C138) with nearly identical size was studied at room temperature employing steady-state and time-resolved fluorescence anisotropy techniques in series of alcohols and alkanes. Experimental observations indicate faster rotation of C138 compared to the other two dyes in alcohols and a faster rotation of C522B than C307 in alkanes. The dielectric friction theories of Nee-Zwanzig (NZ) and van der Zwan-Hynes (ZH) were employed to estimate the friction experienced by the probes in alcohols, in addition to the mechanical friction calculated using Stokes-Einstein-Debye (SED) hydrodynamic with slip boundary condition and Dote-Kivelson-Schwartz (DKS) quasihydrodynamic theories. The observed reorientation times for the three probes do not follow the trend predicted by dielectric friction theories of NZ and ZH. The dipole moments determined from solvatochromic techniques were found to be different for the three probes.

J. R. Mannekutla · S. R. Inamdar (✉)
Laser Spectroscopy Programme, Department of Physics,
Karnatak University,
Dharwad 580 003, India
e-mail: him_lax3@yahoo.com

B. G. Mulimani
Gulbarga University,
Gulbarga 585 106, India

M. I. Savadatti
Karnataka State Council for Higher Education,
Bangalore 560 001, India

Present Address:
J. R. Mannekutla
Radboud University,
Nijmegen, The Netherlands

Keywords Rotational dynamics · SED hydrodynamic theory · Dielectric friction theories · Electrostriction effect

Introduction

Rotational dynamics in liquids is of great relevance that affords a direct probe of frictional coupling between a dissolved solute and its milieu. The molecules in liquid phase possess both the proximity and the mobility to interact with one another and lead to a strong posture on the photophysical changes of the probe molecule. Several experimental, theoretical and computational approaches have been used to study this problem [1–3]. Majority of scientific literature on this topic has centered on two kinds of probes viz., nonpolar and polar. Nonpolar probes, in polar and/or nonpolar solvents are used to understand the influence of solute to solvent size ratio and of solute shape on the friction experienced by the probe molecule and to test the validity of hydrodynamic and quasihydrodynamic theories [4–24]. The friction experienced in this case is purely mechanical dominated by short-range repulsive forces between the molecules. On the other hand, polar and charged molecules in polar solvents are used to understand the long-range electrostatic interactions between the solute and solvent, which are charge-dipole or dipole-dipole in nature [25–43]. A polar molecule rotating in a polar solvent experiences hindrance due to dielectric friction (ζ_{DF}) in addition to the mechanical (ζ_M) or hydrodynamic friction. In general, dielectric and mechanical contributions to the friction are not separable as they are linked due to electrohydrodynamic coupling [32, 44–48]. Despite this nonseparability, it has been a common practice to approximate the total friction experienced by

the probe molecule as the sum of mechanical and dielectric friction components, i.e.,

$$\zeta_{Total} = \zeta_M + \zeta_{DF} \quad (1)$$

Mechanical friction can be modeled using both hydrodynamic [49] and quasihydrodynamic [44, 50] theories. Dielectric friction, on the other hand, can be modeled using continuum theories of the Nee-Zwanzig (NZ) [51], the Alavi-Waldeck (AW) [52] and the van der Zwan-Hynes (ZH) [53] models. A molecular simulation study by Kumar and Maroncelli [48] showed that the mechanical and dielectric contributions to the friction are not separable in any useful way. They studied the iodinelike diatomic molecule, in polar solvents viz., acetonitrile and methanol as function of the solute dipole moment in the range of 0–6.4 D, in which the cross correlation between mechanical and dielectric friction is not negligible, but is almost equal in magnitude to the dielectric friction contribution with a negative sign. Hence, the net friction is smaller than that may result from a simple addition of individual mechanical and dielectric contributions. Dutt and Raman [40] studied the rotational friction experienced by three structurally similar polar molecules coumarin 6 (C6), coumarin 7 (C7) and coumarin 30 (C30) in series of alcohols and alkanes by maintaining the mechanical component of the friction alike, which was confirmed by more or less the same reorientation times obtained in alkanes. The observed dielectric friction contribution could not predict the experimental trend even in a qualitative way and was termed as the failure of point source dielectric friction theories, which fail to capture the electronic properties in a sufficiently realistic way.

The present study reports the study of time-resolved fluorescence of three polar probes: coumarin 522B (C522B), coumarin 307 (C307) and coumarin 138 (C138) (molecular structures are shown in Fig. 1) using steady-state spectrofluorometry and time-correlated single photon counting technique. In these coumarins, the two free substituents at 6 and 7 positions, methyl and ethylamino in case of C307, compared with the analogous model substrate C522B, wherein, there is no free substituent, are joined by ends to form piperidino moiety. Studies of these piperidine-fused coumarins have highlighted their potential as thymine dimer photosensitizers and have also been found to act via the DNA gyrase pathway in their antibacterial activity [54]. These two probes are looked upon as polar due to the presence of electron donating amino group and electron withdrawing -CF_3 group. This -CF_3 group is replaced by an alkyl group in C138 rendering it less polar compared to C522B and C307. It is also observed that the ground and excited state dipole moments are different for these probes. Thus rotational diffusion study of these probes in polar solvents is likely to enhance our understanding of the influence of dipole moments on the dielectric friction.

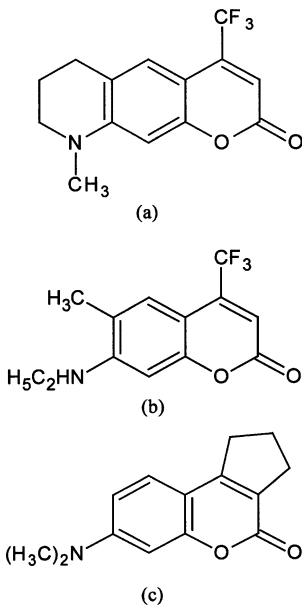

Fig. 1 Molecular structures of **a** C522B, **b** C307 and **c** C138

Experimental

The probes C522B, C307 and C138 (Radiant Dyes Laser GmbH, Germany) were used as received. All the solvents employed in this study were of highest available purity (Fluka, Germany) and were used as such. The absorption and emission spectra of these probes were obtained using UV/vis absorption spectrophotometer (Hitachi, U-2800) and fluorescence spectrophotometer (Hitachi, F-2000), respectively. The solutions of C522B and C307 were excited at 410 nm and those of C138 were excited at 375 nm. All the measurements were performed at 298 K. Rotational reorientation times of these coumarins were determined using the steady-state fluorescence depolarization technique, described elsewhere [23]. For vertical excitation, the steady-state fluorescence anisotropy can be expressed as [18, 55]

$$< r > = \frac{I_{||} - GI_{\perp}}{I_{||} + 2GI_{\perp}} \quad (2)$$

where $I_{\|}$ and $I_{\perp}$ denote the components of fluorescence intensities parallel and perpendicular with respect to the direction of polarization of the exciting beam. G is an instrumental factor that corrects for the polarization bias in the detection system and is given by

$$G = \frac{I_{HV}}{I_{HH}} \quad (3)$$

where I_{HV} is the fluorescence intensity when the excitation polarizer kept horizontal and the emission polarizer vertical

and I_{HH} is that when both the polarizers are maintained horizontal. If both anisotropy and fluorescence, decay as single exponentials then the reorientation time, τ_r, is given by [55]

$$\tau_r = \frac{\tau_f}{(r_0/ < r > -1)} \quad (4)$$

where τ_f is the fluorescence lifetime and r_0 is the limiting anisotropy when all the rotational motions are frozen (measured at -60±2°C using glycerol solutions of the probes). The fluorescence lifetimes were determined using time domain fluorescence spectrometer employing time correlated single photon counting technique (TCSPC) described in detail elsewhere [23]. In brief, a diode pumped millennia V CW laser (Spectra Physics, 532 nm) was used to pump the mode-locked Ti-Sapphire laser (Tsunami, Spectra Physics) operated at 82 MHz. Pulses of 820 nm and 750 nm served as fundamental wavelengths from the Ti-Sapphire laser and were passed through the pulse picker (Spectra Physics, 3980 2S) to pick out 4 MHz pulses. The corresponding second harmonics (410 and 375 nm) were used to excite the samples. The photons emitted from the sample are detected by a high gain Hamamatsu micro channel Plate Photomultiplier tube (R3809U MCP-PMT) at magic angle (54.7^0) after being passed through the monochromator and was processed through a constant fraction discriminator (CFD), a time-to-amplitude converter (TAC) and a multichannel analyzer (MCA). The instrument response function of this system is ~52 ps. The fluorescence decay obtained was further analyzed by using IBH (UK) software (DAS-6).

The reorientation times (τ_r) of coumarins in alcohols were also measured by time-resolved fluorescence depolarization method with TCSPC system [56, 57], wherein the samples of C522B and C307 were excited at 408 nm and those of C138 at 375 nm using a picosecond diode laser (IBH, UK, NanoLED) in an IBH Fluorocube apparatus. In order to obtain the fluorescence anisotropy decay, the analyzer was rotated at regular intervals to get perpendicular [$I\perp(t)$] and parallel [$I_{\parallel}(t)$] components. The same IBH DAS-6 software was used here too to analyze the anisotropy data. All the decays were fitted with a single exponential function with χ^2 lying between 1 and 1.2. The instrument response for the above system is ~90 ps.

Results and discussion

The steady-state absorption and fluorescence spectra of the selected probes are shown in Fig. 2. The reorientation times of C522B, C307 in alcohols and alkanes and of C138 in alcohols only (as it is insoluble in alkanes) obtained from

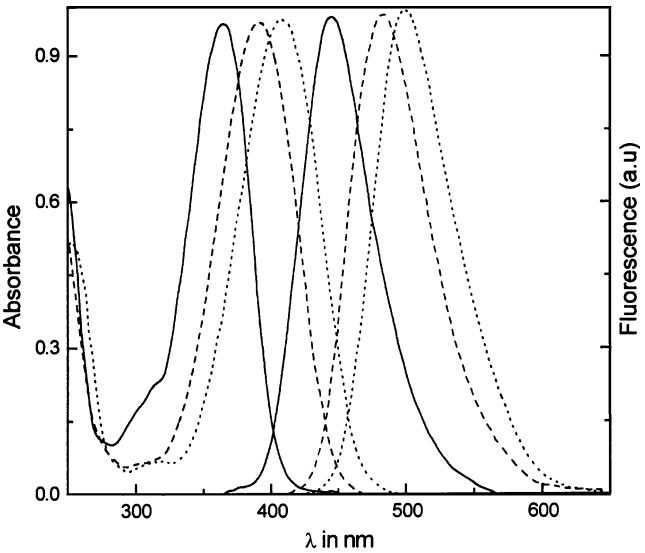

Fig. 2 Absorption and fluorescence spectra of coumarins (C522B …. , C307 ----, C138 ——)

the measured values of <r>, r_0 and τ_f using Eq. 4 are summarized in Tables 1 and 2. The anisotropies (<r>) range from 0.002±0.001 to 0.065±0.002 for various solute-solvent combinations. The steady-state r_0 values for C522B, C307 and C138, respectively, are 0.369±0.004, 0.370±0.003 and 0.365±0.004. The measured time-resolved fluorescence anisotropy decays were found to be single exponentials in all the solvents. The measured time-resolved fluorescence anisotropy parameters of the three probes along with rotational correlation times (τ_r) are summarized in Table 3 and typical fluorescence anisotropy decays of C307 are shown in Fig. 3. τ_r values obtained from steady state and time resolved anisotropy measurements agree fairly well and r_0 is noted to be 9% smaller than those from steady state measurements. A comparison of τ_r values obtained in alkanes show that C522B rotates faster than C307 from heptane through hexadecane. In alcohols, the probe C138 experiences lowest mechanical friction among the three probes. The dissimilar interactions in case of C522B and C138 in alcohols points towards the presence of two different groups (-CF_3 and alkyl) with contradicting properties. The normalized rotational reorientation times (at unit viscosity) are smaller in alkanes compared to alcohols, suggesting that the probes C522B and C307 rotate faster in alkanes compared to alcohols (Table 4). The reorientation times of these three probes thus obtained in alcohols follow the trend $\tau_r^{C307} > \tau_r^{C522B} > \tau_r^{C138}$.

Hydrodynamic model

The Stokes-Einstein-Debye (SED) hydrodynamic theory relates the reorientation time (τ_r) to the macroscopic

Table 1 Steady-state anisotropy (<*r*>), fluorescence lifetime (τ_f) and rotational reorientation time (τ_r) of coumarins in alcohols at 298 K. The maximum error in the fluorescence life times is less than ±50 ps

Solvents	η/mPa s[a]	C522B			C307			C138		
		<*r*>	τ_f / ns	τ_r / ps	<*r*>	τ_f / ns	τ_r / ps	<*r*>	τ_f / ns	τ_r / ps
Methanol	0.55	0.004±0.001	4.87	53±13	0.003±0.001	5.10	42±14	0.003±0.001	3.63	30±10
Ethanol	1.08	0.006±0.001	5.02	83±14	0.006±0.001	5.12	84±14	0.006±0.002	3.63	61±20
Propanol	1.95	0.009±0.001	5.05	126±14	0.011±0.002	5.13	157±29	0.009±0.002	3.64	92±20
Butanol	2.59	0.011±0.002	5.08	156±28	0.016±0.002	5.14	232±29	0.011±0.001	3.64	113±10
Pentanol	3.51	0.013±0.002	5.09	186±29	0.021±0.003	5.14	309±44	0.015±0.003	3.64	156±31
Hexanol	4.57	0.017±0.002	5.09	246±29	0.027±0.002	5.14	405±30	0.020±0.002	3.65	212±21
Heptanol	5.97	0.022±0.003	5.10	323±44	0.034±0.003	5.15	521±46	0.025±0.002	3.65	268±21
Octanol	7.63	0.027±0.002	5.10	403±30	0.041±0.003	5.15	642±47	0.035±0.004	3.68	390±45
Nonanol	9.59	0.033±0.003	5.10	501±46	0.051±0.003	5.18	828±49	0.037±0.002	3.74	422±23
Decanol	11.74	0.042±0.003	5.12	658±47	0.065±0.002	5.18	1,104±34	0.047±0.003	3.77	477±35

[a] Viscosity data is from Ref. [23]

viscosity of the solvent (η), according to which, τ_r, is given by [49]

$$\tau_r = \frac{\eta V}{kT}(fC) \tag{5}$$

where V is the van der Waals volume of the solute. k and T are the Boltzmann constant and absolute temperature, respectively. f is referred to as a shape factor and is well specified. For nonspherical molecules, $f > 1$ and the magnitude of deviation of f from unity describes the degree of the nonspherical nature of the solute molecule. C, is the boundary condition parameter that signifies the extent of coupling between the solute and the solvent [58]. The shapes of the solute molecules are usually incorporated into the model by treating them as either symmetric or asymmetric ellipsoids. In the two limiting cases of hydrodynamic stick and slip for a nonspherical molecule, the value of C follows the inequality, $0 < C \leq 1$ and the exact value of C is determined by the axial ratios of the probe.

The limiting values of the reorientation times using SED theory with stick and slip boundary conditions were calculated as follows: Based on the van der Waals increments method [59], the molecular volumes of C522B, C307 and C138 were determined to be 223 Å^3, 217 Å^3 and 210 Å^3, respectively. The longest end-to-end distance was taken as the long axis ($2a$) of the molecule. The thickness of the probes (c) was taken, as suggested by Waldeck and Fleming [60] for an aromatic molecule giving a half axis of 1.9 Å. The axis perpendicular to the long axis i.e., the short in-plane axis was obtained using the expression

$$V = \frac{4\pi}{3}abc \tag{6}$$

where V corresponds to the volume, a, b and c being the half-axes. The estimated axial radii and the van der Waals volumes of the probes are given in Table 5. All the three probes are modeled as asymmetric ellipsoids [40]. The friction coefficients with stick boundary condition along the

Table 2 Steady-state anisotropy (<*r*>), fluorescence lifetime (τ_f) and rotational reorientation time (τ_r) of coumarins in alkanes at 298 K for C522B and C307. The maximum error in the fluorescence life times is less than ±50 ps

Solvents	η/mPa s[a]	C522B			C307		
		<*r*>	τ_f / ns	τ_r / ps	<*r*>	τ_f / ns	τ_r / ps
Pentane	0.23	–	–	–	0.003±0.001	4.23	35±12
Hexane	0.29	–	–	–	0.003±0.001	4.28	35±12
Heptane	0.41	0.002±0.001	3.98	22±11	0.004±0.001	4.37	48±12
Octane	0.52	0.003±0.001	4.11	34±11	0.004±0.001	4.51	49±12
Nonane	0.66	0.004±0.001	4.17	46±12	0.005±0.001	4.63	63±13
Decane	0.84	0.005±0.001	4.20	58±12	0.006±0.001	4.60	76±13
Dodecane	1.35	0.006±0.001	4.26	70±12	0.007±0.002	4.79	92±26
Tridecane	1.55	0.007±0.001	4.31	83±12	0.008±0.002	4.80	106±27
Pentadecane	2.81	0.009±0.001	4.38	110±12	0.009±0.002	4.80	120±27
Hexadecane	3.07	0.010±0.001	4.52	126±13	0.010±0.002	4.86	135±27

[a] Viscosity data is from Ref. [23]

Table 3 Fluorescence anisotropy decay parameters of coumarins in alcohols at 298 K

Solvents	η/mPa s[a]	C522B		C307		C138	
		$<r_0>^a$	τ_r / ps	$<r_0>^a$	τ_r / ps	$<r_0>^a$	τ_r / ps
Butanol	2.59	0.338	150±25	0.352	213±32	–	–
Pentanol	3.51	0.348	179±28	0.350	286±28	0.330	136±16
Hexanol	4.57	0.369	240±35	0.362	391±35	0.345	198±20
Heptanol	5.97	0.375	311±30	0.371	492±39	0.342	235±30
Octanol	7.63	0.365	395±25	0.373	618±40	0.358	350±32
Nonanol	9.59	0.370	480±38	0.358	786±72	0.362	390±18
Decanol	11.74	0.376	630±40	0.373	1,061±65	0.365	437±29

[a] ±10%

three axes were obtained by interpolating the numerical tabulations of Small and Isenberg [61] while those with a slip boundary condition were obtained from those of Sension and Hochstrasser [62]. From the friction coefficients ζ_i, the diffusion coefficients D_i were calculated using the relation

$$D_i = \frac{kT}{\zeta_i} \tag{7}$$

through which the reorientation times were obtained using the equation [1]

$$\tau_r = \frac{1}{12}\left[\frac{4D_1 + D_2 + D_3}{D_1D_2 + D_2D_3 + D_3D_1}\right] \tag{8}$$

with the assumption that the transition dipole is along the long axis (Fig. 4). The reorientation times calculated with stick and slip boundary conditions together with the shape factor, f and C_{slip}, are tabulated in Table 5. It may be noted that, τ_r/η values are nearly equal for all the three probes studied.

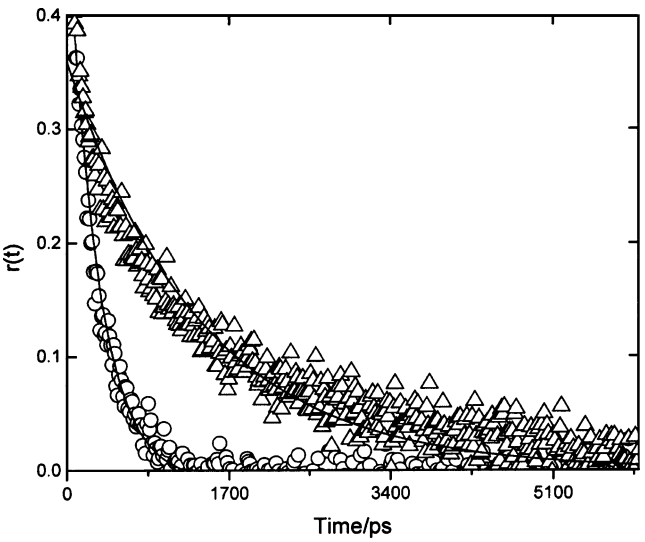

Fig. 3 Fluorescence anisotropy decay of C307 in pentanol (O) and decanol (Δ) with the fitted curves

Figure 5 gives a plot of τ_r vs. η for all the three molecules in alcohols and for C522B and C307 in alkanes along with the stick and slip lines. Note that the experimentally measured reorientation times for the three probes lie between slip and stick hydrodynamics in case of alcohols. However, in alkanes we observe that, as the size of the solvent molecule becomes equal to and larger than the size of the solute molecule, the probe molecules experience a reduced friction. For C522B, the experimental τ_r values are higher than the slip hydrodynamics by a factor of 3.7 to 4.6 from heptane (V=130 Å^3) to decane (V=181 Å^3), whereas from dodecane (V=215 Å^3) to hexadecane (V=283 Å^3) it is from 2.6 to 3.6. An interesting feature to be noted is that, in case of C307, for a ratio of van der Waals volume of the solvent to probe (V_s/V_p) <1 (i.e., from pentane to decane), the probe is experiencing higher friction following stick hydrodynamics and from dodecane to hexadecane the probe experience a reduced friction as the ratio of V_s/V_p increases from 1 to 1.3. Benzler and Luther [21] measured the reorientation times of biphenyl (V=150 Å^3) and *p*-terphenyl (V=221 Å^3) in *n*-alkanes, and observed a nonlinearity in the plot of τ_r vs. η from decane onwards in case of biphenyl and from tetradecane onwards, in the case of *p*-terphenyl. Singh [63] studied reorientation times of the probe neutral red (V=234 Å^3) which experienced a reduced friction from tetradecane to hexadecane following subslip behavior. Note that C522B and C307 have almost identical volumes as compared to neutral red and *p*-terphenyl and thus a similar trend of rotational relaxation in alkanes may be expected. From the logarithmic fits of the data, the relationship between τ_r and η for the three probes in alkanes and alcohols

Table 4 The relation between τ_r and η obtained from the logarithmic fits of data in alkanes and alcohols for the three coumarins

Solute	Alkanes	Alcohols
Coumarin 522B	$(50\pm3)\eta^{(0.77\pm0.07)}$	$(87\pm4)\eta^{(0.81\pm0.03)}$
Coumarin 307	$(72\pm4)\eta^{(0.54\pm0.03)}$	$(80\pm2)\eta^{(1.00\pm0.01)}$
Coumarin138	–	$(52\pm2)\eta^{(0.92\pm0.03)}$

Table 5 Properties of solutes used in the study

Solute	Axial radii/Å^3	V/Å^3	β^a	θ	f	C_{slip}	$\tau_r\eta^{-1}$/ps (mPa s)$^{-1}$		μ_g /D	μ_e /D
							Slip	Stick		
Coumarin 522B	6.1×4.6×1.9	223	1.03	13	1.85	0.15	15	100	2.47[b]	5.15[b]
Coumarin 307	6.3×4.3×1.9	217	1.00	13	1.91	0.18	18	101	1.82[b]	4.50[b]
Coumarin 138	6.5×4.1×1.9	210	0.97	14	1.98	0.22	22	101	2.20[c]	3.42[c]

[a] β is the volume correction factor, defined as the ratio of the volume of the solute to the average volume of the three solutes.

[b] from the ref [64]

[c] from the ref [65]

were obtained and summarized in Table 5. It may be inferred from the Table that these probes follow different correlations with viscosity in alkanes and alcohols. The degree of nonlinearity is not significant in case of alcohols as compared to the alkanes. However, there is little or no theoretical justification for these fits and thus may be considered to be purely empirical in nature.

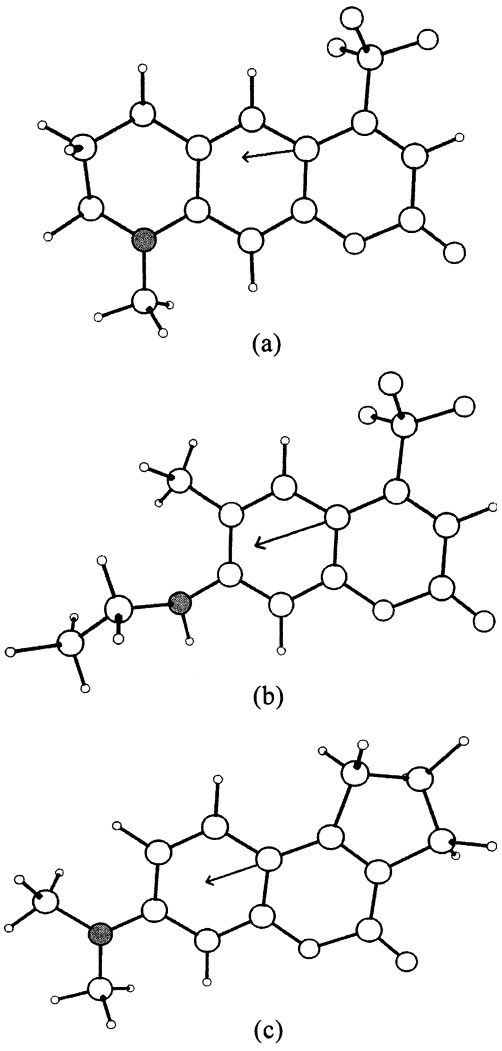

Fig. 4 The B3LYP/6-31 g* optimized structures of the coumarins **a** C522B **b** C307 and **c** C138 along with the directions of transition moment

The hydrodynamic theories take only the size of the solute molecules into consideration and not that of the solvent molecule, while the quasihydrodynamic theories of Geirer-Wirtz (GW) [50] and Dote-Kivelson-Schwartz (DKS) [44] account for the friction experienced by the probe molecule considering not only the size of the solute but also that of the solvent. In the first place, the GW theory is used to calculate the parameters σ and C_0 using the equations

$$\sigma = \left[1 + 6\left(\frac{V_s}{V_p}\right)^{1/3} C_0\right]^{-1}, \tag{9}$$

where

$$C_0 = \left\{\frac{6\left(V_s/V_p\right)^{1/3}}{\left[1 + 2\left(V_s/V_p\right)^{1/3}\right]^4} + \frac{1}{\left[1 + 4\left(V_s/V_p\right)^{1/3}\right]^3}\right\}^{-1} \tag{10}$$

with V_s and V_p being the volumes of the solvent and probe, respectively. The expression for C_{GW} is given by

$$C_{\mathrm{GW}} = \sigma C_0. \tag{11}$$

Nevertheless, the GW theory oversees the relatively poor physical contact between the probe and the solvent arising due to the cavities or free spaces created by the solvent around the probe molecule.

The coupling parameter C_{GW}, varies from 0.17 to 0.29 for the present probes in alcohols, while it is 0.15 and 0.21 for C522B and C307 in alkanes, respectively. Though the GW theory is able to mimic the nonlinear profile of τ_r vs. η, it clearly underestimates the average friction experienced by the probes by factors of 2.9, 4.1 and 2.3 in alcohols for C522B, C307 and C138, respectively. In alkanes, it underestimates that by a factor of 3.2 to 4.8 in case of C522B and C307. It is also noted that the probes experience reduced friction as the size of the solvent increases. A number of

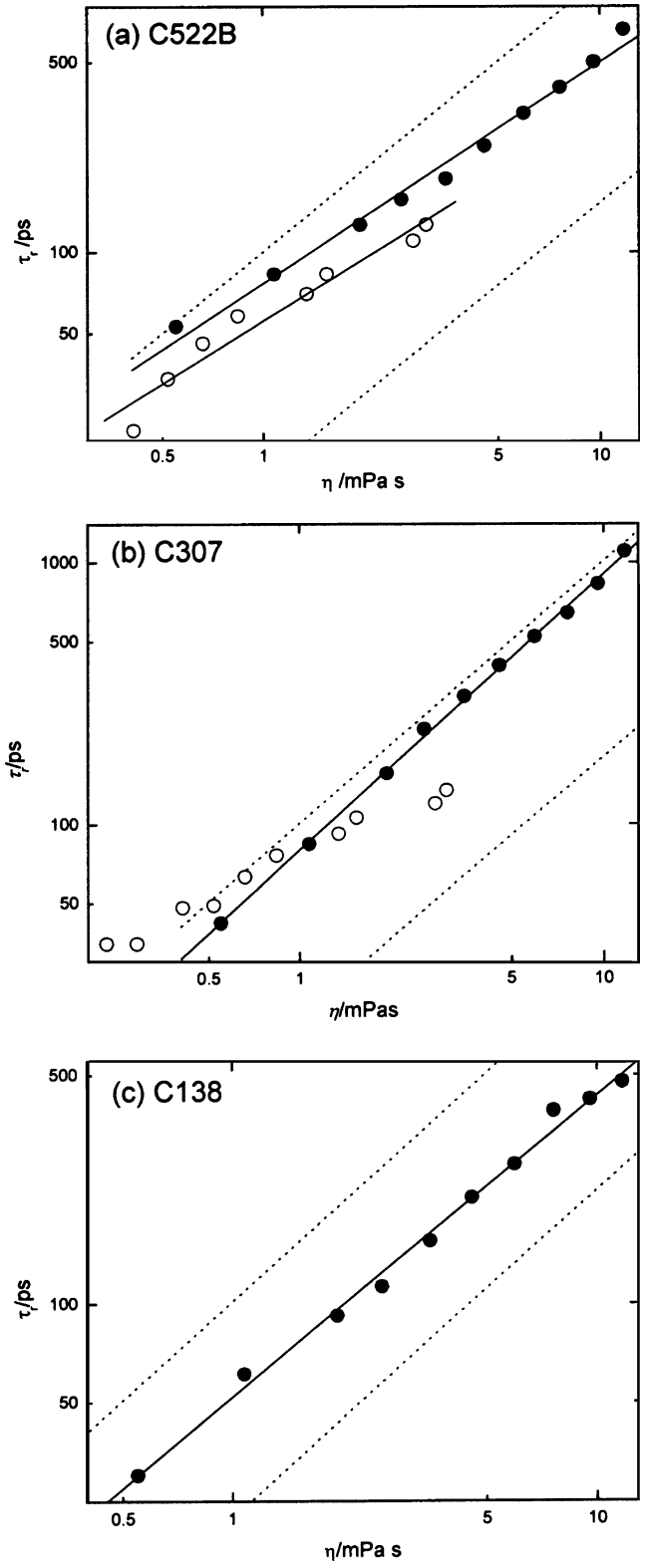

Fig. 5 A plot of τ_r vs. η for the three coumarins in alcohols (●) and in alkanes (○) in case of C522B and C307. Dotted lines above and below the experimental data, respectively, represent theoretical stick and slip limits

reports [7–9, 13, 15, 16] noted faster rotation of many probes in alcohols when compared to alkanes, which has been explained as due to higher free volumes in alcohols compared to alkanes based on DKS theory. The coumarins studied here would have rotated faster in alcohols compared to alkanes in the absence of electrical interactions. However, an opposite trend, observed experimentally, indicates the presence of electrical interactions [40]. Hence, to evaluate the dielectric friction quantitatively, the contribution due to mechanical friction must be estimated with a reasonable degree of accuracy. The SED theory with slip hydrodynamic boundary condition is often used to calculate the mechanical friction in case of medium-sized solute molecules. It may be recalled that, in the present study the solvent size increases by more than 5 times from methanol to decanol and thus it may be appropriate to invoke DKS quasihydrodynamic theory when size effect is taken into account. According to DKS theory the solute-solvent coupling parameter, C_{DKS} is given by

$$C_{DKS} = (1 + \gamma/\phi)^{-1}, \tag{12}$$

where γ/ϕ is the ratio of the free volume available for the solvent to the effective size of the solute molecule, with

$$\gamma = \frac{\Delta V}{V_p}\left[4\left(\frac{V_p}{V_s}\right)^{2/3} + 1\right], \tag{13}$$

and ϕ is the ratio of the reorientation time predicted by slip hydrodynamics to the stick prediction for a sphere of the same volume. ΔV is the smallest volume of free space per solvent molecule and some discretion must be applied while calculating this term [15, 20, 31]. It is empirically related to the solvent viscosity, the Hilderbrand-Batchinsky parameter B and the isothermal compressibility k_T of the liquid by

$$\Delta V = Bk_T\eta kT \tag{14}$$

Since the Frenkel hole theory and the Hilderbrand treatment of solvent viscosity were developed for regular solutions [15], Eq. 14 may not be a valid measure of the free space per solvent molecule for associative solvents like alcohols and polyalcohols. Hence, for alcohols ΔV is calculated using

$$\Delta V = V_m - V_s \tag{15}$$

where V_m is the solvent molar volume divided by the Avogadro number.

Evaluation of dielectric friction contribution demands estimation of the mechanical friction experienced by the probes with a reasonable degree of accuracy. The mechanical friction calculated using DKS theory contributes about 10–20% to the total friction experienced by the probes C522B and C307 and about 25–34% in case of C138 in

alcohols. Since the DKS theory predicts the friction on the probe molecule, taking into consideration the relative size of the probe and solvent as well as the free volume of the solvent, the friction estimated from DKS theory be necessarily included in the calculations though it underestimates the experimentally observed trend by a factor of 5.64 to 7.57, 5.25 to 9.60 and 2.97 to 3.98, respectively, for C522B, C307 and C138. The mechanical friction calculated using slip hydrodynamics did not vary considerably from that estimated by GW theory. Hence, the mechanical friction calculated using slip hydrodynamics is taken, which accounts for about 15–30% of the total friction experienced by C522B and C307 and about 39–55% in case of C138 in alcohols. Mechanical friction experienced by coumarins in alcohols was also estimated from the experimentally observed relationship of τ_r and η in alkanes. It has been opined that alkanes offer more mechanical friction to the rotating probe than alcohols as observed from numerous diffusion studies of nonpolar probes [40]. In the present case, the mechanical friction experienced by the C522B and C307 in alkanes is about 30–55% and 37–47% more than that calculated using slip hydrodynamic theory, while it is about 32–68% and 45–52% with DKS theory, respectively.

Dielectric friction

One of the important mechanisms that hinders the rotation of the polar molecules in polar solvents is dielectric friction. Equation 1 implies that the difference between total friction and mechanical friction can be approximated as contribution due to dielectric friction. Two theoretical models were used to assess the dielectric friction contribution.

The Nee-Zwanzig (NZ) [51] theory that assumes the solute to be a point dipole located inside a spherical cavity of radius a and the solvent as a continuous dielectric medium characterized by a frequency dependent dielectric constant was used in the present study. If μ is the dipole moment of the solute, ε_0 and ε_∞ are the zero- and high-frequency dielectric constants of the solvent, respectively, then the dielectric friction, τ_{DF} experienced by the solute in the limit of zero-frequency is given by [51, 64]

$$\tau_{DF} = \frac{\mu^2}{9a^3kT}\frac{(\varepsilon_\infty+2)^2(\varepsilon_0-\varepsilon_\infty)}{(2\varepsilon_0+\varepsilon_\infty)^2}\tau_D \tag{16}$$

where τ_D is the Debye relaxation time of the solvent. The excited state dipole moments and dielectric properties in alcohols using Eq. 16 were obtained from our earlier study of C522B and C307 [65], while for C138, they are taken from Ref. [66]. Two different values of a signifying were used to calculate τ_{DF} using NZ theory. The first value of a was taken from the van der Waals volume of the solutes, treating them as spherical molecules and the second value was derived from the half length of the long axis as given in Table 5. However, the normal practice is to model the molecule as a sphere and determine its radius from the molecular volume [27, 55]. From the experimentally measured reorientation time, τ_{DF} was obtained using the relations, $\tau_{DF} = \tau_r^{Expt} - \tau_r^{Slip}$ and $\tau_{DF} = \tau_r^{Expt} - \tau_r^{DKS}$ for all the three coumarins whereas, $\tau_{DF} = \tau_r^{Expt} - \tau_r^{Alkanes}$ is used additionally in case of C522B and C307. To compare the theoretically calculated dielectric friction with that obtained experimentally, τ_{DF} was plotted as a function of A in Fig. 6 for all the probes using different relations of dielectric frictions, where

$$A = \frac{(\varepsilon_\infty+2)^2(\varepsilon_0-\varepsilon_\infty)}{(2\varepsilon_0+\varepsilon_\infty)^2}\tau_D. \tag{17}$$

It is clear from the figure that the NZ theory for both values of a overestimates the dielectric friction contribution. The dipole moments obtained from the slopes of the plots of τ_{DF} vs. A for the experimentally observed dielectric friction, are shown in Table 6. If excited state dipole moments obtained from solvatochromic shift method in alcohols are considered, then the dielectric friction experienced by the probes is expected to follow the order $\tau_{DF}^{C522B} > \tau_{DF}^{C307} > \tau_{DF}^{C138}$. However, it is surprising to note that the experimental trends followed are: $\tau_{DF}^{C307} > \tau_{DF}^{C522B} > \tau_{DF}^{C138}$, $\tau_{DF}^{C307} \approx \tau_{DF}^{C522B} < \tau_{DF}^{C138}$ and $\tau_{DF}^{C307} > \tau_{DF}^{C522B}$ when dielectric contributions, respectively, with slip, DKS and alkanes, are considered.

A semiempirical method for finding dielectric friction proposed by van der Zwan and Hynes (ZH) [53], relates the dielectric friction experienced by a solute in a solvent, to Stoke's shift ($\Delta\nu$) and solvation time, τ_s as,

$$\tau_{DF} = \frac{\mu^2}{(\Delta\mu)^2}\frac{hc\ \Delta\nu}{6kT}\tau_s \tag{18}$$

where $\Delta\mu$ is the difference between dipole moment of the solute in the ground and excited states. $\Delta\nu$ values for C522B and C307 were taken from Ref. [65] and for C138, it varied from 4,821–5,207 cm^{-1} in alcohols. The solvation time is approximately related to the solvent longitudinal relaxation time, $\tau_L = \tau_D(\varepsilon_\infty/\varepsilon_0)$ and is relatively independent of the solute properties [67–71]. The observed dielectric friction τ_{DF}, obtained using Eq. 18 was plotted as a function of $\Delta\nu\tau_L$ (Fig. 7). The experimentally observed dielectric frictions using the three relations (as was done in case of NZ model) have also been used here and are plotted in the figure. It is observed that the theoretically calculated dielectric friction using ZH theory overestimates the experimentally observed dielectric friction contribution as was also noted in the case of NZ theory. $\mu^2/(\Delta\mu)^2$ values obtained from the slopes of the plots of τ_{DF} vs. $\Delta\nu\tau_L$ are summarized in Table 7 along

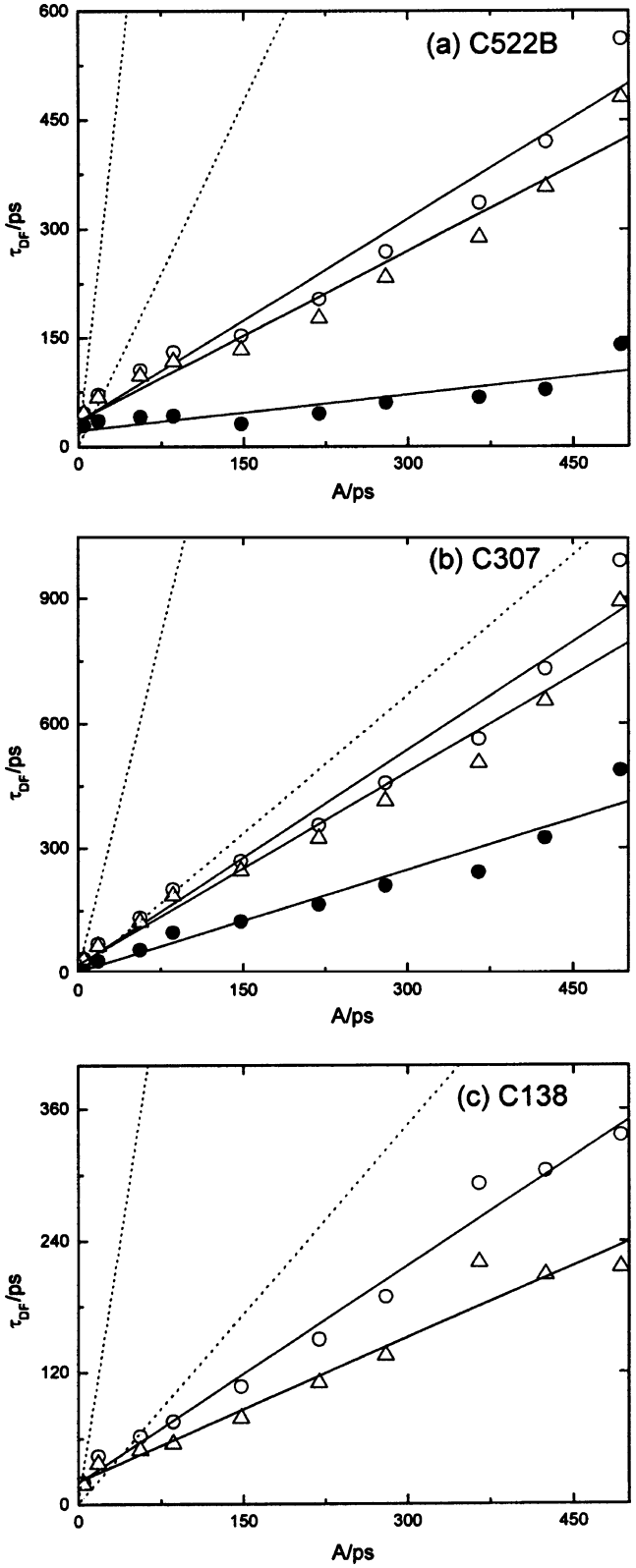

Fig. 6 A plot of experimentally measured dielectric friction τ_{DF} as a function of A. τ_{DF} was obtained from the experimentally measured reorientation times using three different methods $\tau_{DF} = \tau_r^{Expt} - \tau_r^{Slip}$, $\tau_{DF} = \tau_r^{Expt} - \tau_r^{DKS}$ in case of all the three coumarins and are plotted as open triangle and circles, respectively, and $\tau_{DF} = \tau_r^{Expt} - \tau_r^{Alkanes}$ is used in case of C522B and C307 with filled circles. The dotted lines are calculated ones using Eq.16. The upper and lower lines correspond to two values of '*a*' as explained in the text

with the experimental values. When compared with $\mu^2/(\Delta\mu)^2$ values calculated from Table 4, one expects the observed trend to be: $\tau_{DF}^{C138} > \tau_{DF}^{C522B} > \tau_{DF}^{C307}$, nevertheless, from the slopes of Fig. 7, it is observed that $\tau_{DF}^{C307} > \tau_{DF}^{C522B} > \tau_{DF}^{C138}$. The $\mu^2/(\Delta\mu)^2$ values are larger by a factor of 52, 5 and 12, respectively, for C138, C307 and C522B with respect to dielectric friction using slip and DKS theories, whereas in case of alkanes it varies from 11 to 61, for C307 and C522B. The large difference in $\mu^2/(\Delta\mu)^2$ values using dielectric friction in alkanes and that obtained with ZH theory may account for the fact that higher mechanical friction offered by the alkanes is much more than the dielectric friction in case of C307 and C522B.

Clearly both the dielectric friction theories fail to predict the observed behavior, even qualitatively. Note that the NZ model predicts a reduced friction for C138 as it has a low excited state dipole moment in comparison with C522B and C307. An opposite trend is predicted by ZH theory, based on their $\mu^2/(\Delta\mu)^2$ and $\Delta\nu$ values and the experimentally observed trend is closer to the predictions of ZH theory. The experimental dipole moment values in alcohols obtained using solvatochromic technique increase with increasing size of probes (Table 5). Thus, it is normal to expect the probe C522B to rotate slowly and consequently experience higher dielectric friction compared to C307 and C138. However, it is interesting to observe a reverse trend where C307 is experiencing higher dielectric friction and rotates about 40% and 50% slower in alcohols from pentanol to decanol as compared to C522 and C138. The reason for this may be that the nitrogen atom is part of secondary amino group in C307 while it is part of the tertiary amino group in C522B. In such case, the former can

Table 6 Excited state dipole moments obtained from the slope of the plot τ_{DF} vs. *A* using NZ theory

Solute	μ_e/D[a]	μ_e/D[b]
Coumarin 522B	4.1±0.2 (1.8±0.1[c])	8.5±0.6 (3.7±0.3[c])
Coumarin 307	5.6±0.3 (3.9±0.4[c])	12.3±0.9 (8.7±0.6[c])
Coumarin138	3.2±0.2	7.5±0.4

[a] Dipole moments obtained taking van der Waals radius of the probe molecule (*a*)

[b] Dipole moments obtained taking half length of the long axis (*a*)

[c] Dipole moment values obtained from the slopes of τ_{DF} vs *A* in case of Alkanes

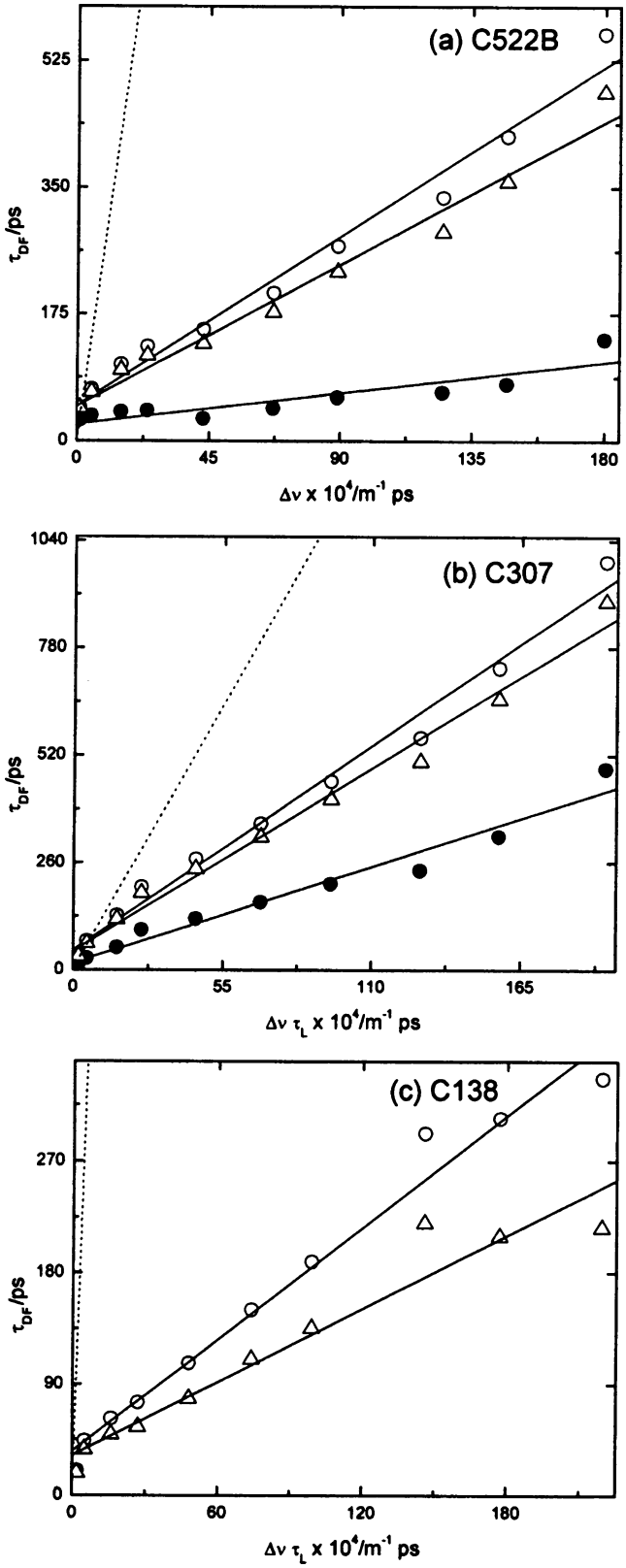

◀ **Fig. 7** A plot of experimentally measured dielectric friction τ_{DF} as a function of $\Delta\nu\ \tau_L$, τ_{DF} was obtained from the experimentally measured reorientation times using three different methods i.e., $\tau_{DF} = \tau_r^{Expt} - \tau_r^{Slip}$, $\tau_{DF} = \tau_r^{Expt} - \tau_r^{DKS}$ in case of all the three coumarins and are plotted as open triangle and circles, respectively, and $\tau_{DF} = \tau_r^{Expt} - \tau_r^{Alkanes}$ is used in case of C522B and C307 with filled circles. The dotted lines are calculated ones using Eq. 18

better contribute to hydrogen bonding leading to higher dielectric friction. The dielectric friction contribution in case of two similar probes-neutral and cationic forms of neutral red in series of alcohols, amides and aprotic solvents using NZ and ZH theories has been determined by Dutt et al. [31]. The van der Waals volumes of these two probes (234 and 237 Å^3) are almost equal to those of the present coumarin molecules. Both neutral and cationic forms were found to experience more or less the same friction in alcoholic solvents. Another probe C7 (V=297 Å^3, μ_e=9.6 D) possessing a lower dipole moment compared to C6 (V=303 Å^3, μ_e=12.0 D) was noted to rotate about 20% faster [40]. This was attributed to the -NH group in C7 forming a hydrogen bond with alcohol solvents, which hinders the molecular rotation. However, C30 (V=315 Å^3, μ_e=10.9 D) wherein the -NH group is replaced by the N-CH_3 also experiences the same friction as C7. It was concluded that the friction experienced by C6 and C7 is not due to hydrogen bonding. The previous studies [19, 20, 72] of two structurally similar nonpolar probes DPP and DMDPP in hydrogen bonding solvents also support this reasoning. Incidentally a similar trend is observed in the present study with C522B rotating much faster compared to C307. Also it may be noted that the dipole moment values of C6 and C7 are larger by more than 50% compared to those of C522B and C307. This clearly rules out the possibility of the observed dielectric friction for C522B and C307 arising out of solute-solvent hydrogen bonding.

The disagreement between SED and NZ theories, has led to various improvements in the original NZ description in the recent past. Showing unambiguously that the NZ formalism is only a special case of dielectric continuum predictions of solvation dynamics, Maroncelli [64] noted that the NZ formalism described by Eq. 16 is invalid. His

Table 7 Excited state dipole moments obtained from the slope of the plot τ_{DF} vs. $\Delta\nu\ \tau_L$ using ZH theory

Solute	$\mu/(\Delta\mu)^{2a}$	$\mu/(\Delta\mu)^{2b}$
Coumarin 522B	0.30±0.02 (0.06±0.01[c])	3.69±0.08
Coumarin 307	0.53±0.03 (0.26±0.01[c])	2.82±0.05
Coumarin138	0.15±0.01	7.86±0.22

[a] Obtained from the slope of the plot τ_{DF} vs $\Delta\nu\ \tau_L$

[b] Calculated from the dipole moment values listed in Table

[c] Dipole moment values obtained from the slopes of τ_{DF} vs $\Delta\nu\ \tau_L$ in case of Alkanes

remark is of importance for weakly polar solvents. However, since nuclear polarization is dominant in polar solvents we have used Eq. 16 in the present work to calculate dielectric friction. Alavi and coworkers [32–36] applied the extended charge distribution (AW model) [52] to explain the dielectric friction experienced by a number of polar molecules in polar solvents. This model intended to improve the microscopic effects of dielectric friction for a larger solute molecule and to successfully underscore the fact that the molecules having no permanent dipole moment experience more dielectric friction than those possess it. However, it was unsuccessful in modeling the friction in associative solvents like alcohols. Also, the inseparability of mechanical and dielectric friction [40, 46, 73, 74] could also be one of the prominent reasons for the failure of dielectric friction models. The dielectric contribution calculated using NZ and ZH (both van der Waals radius and length of long axis) overestimate the experimentally observed trend in the present study. The results also show that the probes C522B and C307 rotate faster in alkanes than in alcohols thus ruling out the possibility of dielectric friction, and the observed interaction could be due to "electrostriction" [48]. The possible reason for the electrostriction is explained in terms of solvent molecules that are arranged to maintain electrical interactions with the solute, which are attractive, because of their polar nature. This electrostatic interaction leads to slow diffusion and increase in the density around the solute molecule, thereby increasing the mechanical friction further [40].

Conclusion

The rotational reorientation times of three polar molecules viz., C522B, C307 and C138, with nearly identical volumes, have been measured in series of alcohols and alkanes at room temperature. A coincidental similar rotational reorientation times are observed in case of C522B and C138 in alcohols from propanol to decanol though the molecules have two different groups with contradicting properties. The dipole moments in the ground and excited states are found to be different for all the three probes and increase with probe size. The dielectric friction measured in alcohols indicates that the observed reorientation times of these coumarins did not follow the trends predicted by the theories of NZ and ZH. The probe C522B with higher volume and dipole moment as compared to C307, experiences less friction from pentanol to decanol. Slip hydrodynamic and DKS quasihydrodynamic theories were employed to calculate the mechanical friction. The difference in mechanical friction obtained from DKS and slip is about 25% for C522B and C307 as compared to C138 in alcohols, whereas, it varied in alkanes from around 7-8% for C522B and C307. The dielectric frictions calculated using dielectric friction theories of NZ and ZH, highly overestimates the experimental values, and could not explain the observed trend, even in a qualitative way. The failure of the dielectric friction theories could be due to the inseparability of mechanical and dielectric friction components as the cross correlation, in which the net friction is much smaller than that would be obtained from a simple addition of these two components. This has also been noted in a simulation study [48]. Since the probe C138 behaves in a way similar to that of C522B, as seen from their reorientation times in alcohols, it is clear that similar electrical interactions are involved in case of C138. Hence, the observed faster rotation of C522B and C307 in alkanes compared to alcohols may be attributed to electrostriction effect.

Acknowledgements This work is supported by the grants from the Council of Scientific and Industrial Research (CSIR), New Delhi in the form of a Major Research Project. One of the authors (JRM) is grateful to CSIR for the award of a Senior Research Fellowship. The help of Prof. P. Ramamurthy, National Centre for Ultrafast Processes, Chennai in fluorescence lifetime measurements is gratefully acknowledged. The authors also acknowledge the help of Dr. G.B. Dutt, BARC, Mumbai for his help and encouragement.

References

1. Fleming GR (1986) Chemical applications of ultrafast spectroscopy. Oxford University Press, New York, and references therein
2. Dorfmüller Th, Pecora R (eds) (1987) Rotational dynamics of small and macromolecules. Springer-Verlag, Berlyn
3. DH Waldeck (2000) In: Waluk J (ed), Conformational analysis of molecules in excited states, Wiley-VCH. New York
4. Fleming GR, Knight AEW, Morris JM, Robbins RJ, Robinson GW (1977) Chem Phys Lett 51:399
5. Waldeck DH, Lotshaw WT, McDonald DB, Fleming GR (1982) Chem Phys Lett 88:297
6. Canonica S, Schmid AA, Wild UP (1985) Chem Phys Lett 122:529
7. Phillips LA, Webb SP, Clark JH (1985) J Chem Phys 83:5810
8. Courtney SH, Kim SK, Canonica S, Fleming GR (1986) J Chem Soc, Faraday Trans 82:2065
9. Ben-Amotz D (1987) T W Scott J Chem Phys 87:3739
10. Bowman RM, Eisenthal KB, Millar DP (1988) J Chem Phys 89:762
11. Ben-Amotz D, Drake JM (1988) J Chem Phys 89:1019
12. Kim SK, Fleming GR (1988) J Phys Chem 92:2168
13. Roy M, Doraiswamy S (1993) J Chem Phys 98:3213
14. Jiang Y, Blanchard GJ (1994) J Phys Chem 98:6436
15. Anderton RM, Kauffman JF (1994) J Phys Chem 98:12117
16. Brocklehurst B, Young RN (1995) J Phys Chem 99:40
17. De Backer S, Dutt GB, Ameloot M, De Schryver FC, Mullen K, Holtrup F (1996) J Phys Chem 100:512
18. Dutt GB, Srivatsavoy VJP, Sapre AV (1999) J Chem Phys 110:9623
19. Dutt GB, Srivatsavoy VJP, Sapre AV (1999) J Chem Phys 111:9705
20. Dutt GB, Rama Krishna G (2000) J Chem Phys 112:4676
21. Benzler J, Luther K (1997) Chem Phys Lett 279:333
22. Jas GS, Wang Y, Pauls SW, Johnson CK, Kuczera K (1997) J Chem Phys 107:8800

23. Inamdar SR, Mannekutla JR, Mulimani BG, Savadatti MI (2006) Chem Phys Lett 429:141
24. Mannekutla JR, Ramamurthy P, Mulimani BG, Inamdar SR (2007) Chem Phys 340:149
25. Kivelson D, Spears KG (1985) J Phys Chem 89:1999
26. Templeton EFG, Kenney-Wallace GA (1986) J Phys Chem 90:2896; *ibid* (1986) J Chem Phys 90:5441
27. Simon JD, Thompson PA (1990) J Chem Phys 92:2891
28. Dutt GB, Doraiswamy S, Periasamy N, Venkataraman B (1990) J Chem Phys 93:8498
29. Dutt GB, Doraiswamy S, Periasamy N (1991) J Chem Phys 94:5360
30. Dutt GB, Doraiswamy S (1992) J Chem Phys 96:2475
31. Dutt GB, Singh MK, Sapre AV (1998) J Chem Phys 109:5994
32. Alavi DS, Hartman RS, Waldeck DH (1991) J Chem Phys 94:4509
33. Alavi DS, Hartman RS, Waldeck DH (1991) J Chem Phys 95:6770
34. Hartman RS, Alavi DS, Waldeck DH (1991) J Phys Chem 95:7872
35. Hartman RS, Waldeck DH (1994) J Phys Chem 98:1386
36. Hartman RS, Konitsky WM, Waldeck DH, Chang YJ, Castner EW Jr (1997) J Chem Phys 106:7920
37. M-L Horng, Gardecki JA, Maroncelli M (1997) J Phys Chem A 101:1030
38. Laitinen E, Korppi-Tommola J, Linnanto J (1997) J Chem Phys 107:7601
39. Wiemers K, Kauffman JF (2000) J Phys Chem A 104:451
40. Dutt GB, Raman S (2001) J Chem Phys 114:6702
41. Dutt GB, Rama Krishna G, Raman S (2001) J Chem Phys 115:4732
42. Dutt GB, Ghanty TK (2003) J Phys Chem B 107:3257
43. Dutt GB, Sachdeva A (2003) J Chem Phys 118:8307
44. Dote JL, Kivelson D, Schwartz RN (1981) J Phys Chem 85:2169
45. Hubbard J, Onsager L (1971) J Chem Phys 67:4850
46. Hubbard J (1978) J Chem Phys 69:1007
47. Felderhof BU (1983) Mol Phys 48:1269; *ibid* (1983) Mol Phys 48:1283
48. Kumar PV, Maroncelli M (2000) J Chem Phys 112:5370
49. Debye P (1929) Polar molecules. Dover, New York
50. Gierer A, Wirtz K, Naturforsch Z (1953) A 8:532
51. Nee TW, Zwanzig R (1970) J Chem Phys 52:6353
52. Alavi DS, Waldeck DH (1991) J Chem Phys 94:6196; *ibid* J Chem Phys (1993) 98:3850
53. van der Zwan G, Hynes JT (1985) J Phys Chem 89:4181
54. Kulkarni MV, Kulkarni GM, Lin CH, Sun CM (2006) Cur Med Chem 13:2795
55. Lakowicz JR (1999) Principles of fluorescence spectroscopy, 2nd edn. Kluwer/Plenum, New York
56. Ghosh S, Adhikari A, Mandal U, Dey S, Bhattacharyya K (2007) J Phys Chem C 111:8775
57. Seth D, Chakraborty A, Setua P, Sarkar N (2006) Langmuir 22:7768
58. Hu C-M, Zwanzig R (1974) J Chem Phys 60:4354
59. Edward JT (1970) J Chem Edu 47:261
60. Waldeck DH, Fleming GR (1981) J Phys Chem 85:2614
61. Small EW, Isenberg I (1977) Biopolymers 16:1907
62. Sension RJ, Hochstrasser RM (1993) J Chem Phys 98:2490
63. Singh MK (2000) Photochem Photobiol 72:438
64. Maroncelli M (1997) J Chem Phys 106:1545
65. Mannekutla JR, Mulimani BG, Inamdar SR (2008) Spectrochim Acta Part A 69:419
66. Chandrasekhar K, Naik LR, Suresh Kumar HM, Math NN (2006) Ind J Pure and Appl Phys 44:292
67. Simon JD (1988) Acc Chem Res 21:128
68. Castner EW Jr, Fleming GR, Bagchi B, Maroncelli M (1988) J Chem Phys 89:3519
69. Castner EW Jr, Fleming GR, Bagchi B (1988) Chem Phys Lett 143:270
70. Chapman CF, Fee RS, Maroncelli M (1990) J Phys Chem 94:4929
71. Barbara PF (1988) Acc Chem Res 21:195
72. Dutt GB (2000) J Chem Phys 113:11154
73. Titulaer UM, Deutch JM (1974) J Chem Phys 60:1502
74. Bottcher CFJ, Bordewijk P (1978) Theory of electric polarization, vol II, 78th edn. Elsevier, Amsterdam